

Soil dragging on anchor rods due to settlements

Dijkstra, Siebe; Meinhardt, Guido; De Gijt, Jarit; Bakker, Klaas Jan

Publication date

2017

Document Version

Final published version

Published in

ICSMGE 2017 - 19th International Conference on Soil Mechanics and Geotechnical Engineering

Citation (APA)

Dijkstra, S., Meinhardt, G., De Gijt, J., & Bakker, K. J. (2017). Soil dragging on anchor rods due to settlements. In *ICSMGE 2017 - 19th International Conference on Soil Mechanics and Geotechnical Engineering* (Vol. 2017-September, pp. 1279-1282)

Important note

To cite this publication, please use the final published version (if applicable). Please check the document version above.

Copyright

Other than for strictly personal use, it is not permitted to download, forward or distribute the text or part of it, without the consent of the author(s) and/or copyright holder(s), unless the work is under an open content license such as Creative Commons.

Takedown policy

Please contact us and provide details if you believe this document breaches copyrights. We will remove access to the work immediately and investigate your claim.

SOIL DRAGGING ON ANCHOR RODS DUE TO SETTLEMENTS

Siebe Dijkstra

VolkerInfra, Geo-engineering, The Netherlands, sdijkstra@volkerinfra.nl

Guido Meinhardt

Crux, Geo-engineering, The Netherlands, meinhardt@cruxbv.nl

Jarit de Gijt

Delft University of Technology, Hydraulic Engineering, The Netherlands, J.G.deGijt@tudelft.nl

Klaas Jan Bakker

Delft University of Technology & WAD43, Geo-engineering, The Netherlands, k.j.bakker@wad43.nl

ABSTRACT: The settlement of soil layers on embedded anchor rods may lead to an increased axial load in the rod. The common method of evaluating stresses in anchor rods, according to the Dutch Sheet Piling handbook, better known as CUR 166, implicitly assumes a number of simplifications and assumptions that may in practice lead to a too simplified approach, that is too conservative. Within the context of study for an MSc degree, the main author of this paper has looked into the possibilities to improve the method of evaluation that complies with all codes and is less conservative. The study both looks into drained and undrained conditions for settling clay. Further, the settlement is more explicitly defined as a function of local position at the anchor rod. The method is verified with FEM analysis using Embedded beams, which gave a good corroboration. The method enables to perform an improved design.

Le dépôt de couches de sol sur des tiges d'ancrage encastrées peut entraîner une charge axiale accrue dans la tige. La méthode courante d'évaluation ce cas, selon le manuel néerlandais, d'après CUR 166, iclus un certain nombre de simplifications qui peuvent conduire en pratique à une approche trop simplifiée, trop conservatrice. Dans le cadre de l'étude d'une maîtrise, le principal auteur de cet article a examiné les possibilités d'améliorer la méthode d'évaluation qui est conforme aux codes al et est moins conservatrice. L'étude examine à la fois les conditions drainées et non drainées pour le dépôt de l'argile. En outre, le règlement est plus explicitement défini en fonction de la position locale au niveau de la tige d'ancrage. La méthode est vérifiée par une analyse FEM utilisant des faisceaux embarqués, ce qui a donné une bonne corroboration. Le procédé permet d'effectuer une conception améliorée.

KEYWORDS: Clay, CUR 166, anchor rod deformation, shear strength, settlements, FEM, plastic deformation.

1 INTRODUCTION. FIRST LEVEL HEADING

Anchor rods for soil retaining sheet pile walls in soft soil may, on the longer term be unfavourably subjected to time dependent settlement, i.e due to creep. These settlements, dragging on the embedded anchor rods may lead to straining and with that to an increase of the anchor force. The present method for design according to CUR 166, offers the possibility to model the stresses, based on a simplification to four standard situations, out of which the designer has to choose. Within these schemes the anchor is modelled as a beam on two supports, (the anchor head and the anchor body), that is loaded with a constant lateral load, that represents the settling soil. The method may be regarded as a variant of a rigid-plastic approach, whereas in reality the load may be limited if the settlement of the anchor rod for a part equalizes with the soil. Especially for the inclined anchor rods of grout-anchors this will limit the amount of additional straining of the anchor. This present design method in CUR 166 gives only limited possibilities to versify in the ways to model different situation and this might lead to an overestimation of the actual forces in the anchor rod. This observation was an inducement to have a better look into the possibilities to improve the method of evaluation.

2 THEORY

For the problem of soil dragging on anchor rods, distinction must be made between the way that soil loads the rods and the way in which the rods deform. The limit to the interaction load in clay according to CUR 166 may be calculated with.

$$q_z = s_u \cdot D \cdot (1 + \alpha) \quad (1)$$

Where q_z = the vertical load on the rod per length [kN/m]; s_u = undrained shear strength [kPa]; D = diameter of the rod [m]; α = coefficient of influence.

The CUR 166 defines the value of 5 to the coefficient α , whereas according to literature, see e.g. (Martin & Randolph, 2006) higher values 8 to 11 can be found. The possible underestimation of the drag gave Deltares a reason to perform laboratory tests.

2.1 Laboratory test to verify the maximum drag

To verify the maximum drag, laboratory tests were performed, see, (Lottum, 2010). These tests where done on scale in an oedometer device using T-bars with a limited size using for clay, (Speswhite clay).

Per model test, to start with, the soil was consolidated to achieve the proper undrained shear strength with depth. The T-bar with a length of 50 mm and a diameter of 8 mm is pushed into the soil with a constant speed for a length of 10 mm. The activated force is measured. For numerical verification the parameters of Speswhite clay were established, for the Plaxis HS model, see Table 1.

The tests where numerically verified with Plaxis. With that it was found that although CUR 166 assumes undrained behaviour for clay, with the tests, simulating the dragging due to creep, showed drained behaviour. With that the issue had risen whether the CUR assumption of undrained behavior was proper, for clay, for the long term loading.

Table 1. Speswhite Clay for the HS material model (drained); see (Feddemma, Breedevelde, & Tol, 2010) and (Lottum, 2010).

γ_d/γ_{sat}	E_{50}^{ref}	E_{oed}^{ref}	E_{ur}^{ref}	c'	ϕ'	K_0^{nc}
[kN/m ³]	[kN/m ²]	[kN/m ²]	[kN/m ²]	[kN/m ²]	[°]	[-]
17	1870	1050	12300	0,1	23	0,609

Indeed drained or undrained may make a large difference as the isotropic strength may change to drainage. This is illustrate in Figure 1 for the stresspath in a test; prior to testing, after consolidation the average effective isotropic stress is -87 kPa, combined with a deviator stress of 46 kPa. After that the T-bar is activated and displaced with a test speed. Due to that the stress may change. The average effective stress is a combination of vertical and horizontal stresses according to:

$$p' = \frac{\sigma'_1 + \sigma'_2 + \sigma'_3}{3} \quad (2)$$

If the soil is undrained the isotropic stress may decrease due to activated pore pressures and with that the deviatoric stress may hit the yield envelop at a lower deviatoric stress, whereas for drained soil the isotropic stress may be higher as the yield envelop opens up to the higher compressive stress. For a proper assessment of the soil strength it is vital to know the drainage conditions.

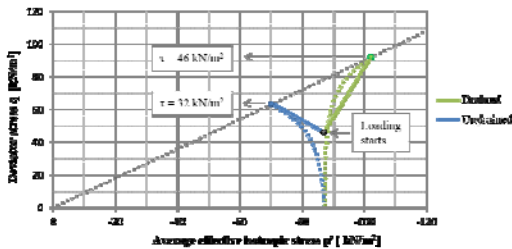


Figure 1: P-q diagram for the stresspath during drained and undrained loading up to failure.

Based on this observation it was concluded that even for the long-term dragging load of clay drained soil conditions must be assumed. Therefore we propose to change the formulation in CUR into Eq 3. Where τ = maximum shear strength at failure [kPa]; f_i = coefficient of influence [-].

$$q_z = \tau \cdot D \cdot (1 + f_i) \quad (3)$$

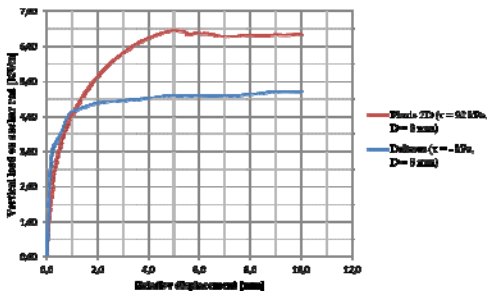


Figure 2: Load displacement curve in which one drained test of the model tests (Deltares) has been simulated with Plaxis 2D.

In Figure 2, the load displacement curve as found in one of the tests is indicated. With the displacement of the anchor, the lateral load increases up to the point that the limiting load is reached. Based on that, the influence factor may be established.

It was concluded that due to the limited dimensions and the low loading rate the soil reaction must be regarded as drained, even while the soil was clay. Although aware of this observation, to correspond to the formulation in CUR, in a first report Deltares has stated the test results as values of s_u , with corresponding values of the coefficient of influence. However in our opinion this may lead to errors, and our proposal is to keep to the physical behaviour and to regard the result as the higher shear strength with corresponding coefficients of influence that corroborate with the values found in literature for this mechanism.

During the testing period, various tests have been performed. A number of these have been evaluated with Plaxis. By

comparing the results, the corresponding values of the coefficient of influence f_i were established. A comparison of the results is given for various testing speeds is (see Figure 3). The lower values of the testing speed, i.e. the longer waiting times are characteristic for autonomous soil settlements due to creep, where drained soil behaviour must be assumed, see (Mayne, 2009). For the testing situation loading speed was varied between 40 mm/day up to 4 mm/month. The latter situation is more characteristic for the situation of long term settlements.

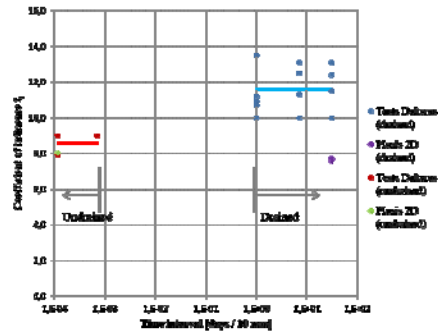


Figure 3: Coefficient of influence plotted against the time interval of drained and undrained failure of Speswhite clay.

Despite the use of equal boundary conditions the model tests showed a large spread in outcome, much larger than was found in the Plaxis results. This difference was attributed to the difficulty of model preparation to repeatedly produce the same initial stresses. The trend in the results in Figure 3 indicates a value for the influence coefficient between 8,6 for undrained and 11,6 for drained conditions, see (Lottum, 2010). For both situation the undrained shear strength was applied to calculate the coefficient of influence. The drained test for that reason show a higher values of f_i , as the drained loading results in a higher drag. In Plaxis 2D the shear strength is modified as a function of the drainage, which leads to a constant value of f_i for both drained and undrained conditions.

After the interaction is established one can focus on the result of the interaction and the effects on the anchor force.

2.2 Deformations of the anchor rod

The settlement curve (w_g) and the subgrade modulus along the anchor are decisive for the loading on the anchor rod, see Figure 4. As the normal profile of settlement due to creep diminishes with depth also the difference in settlement between soil and rod may vary with depth. This load caused may result in deformation of the anchor (w_s). It is the difference between w_s and w_g that is decisive for the load on the rod and the interaction. If $(w_g - w_s) \ll$, the interaction is elastic and may be much lower than the maximum that is calculated using the procedure described in CUR 166. On various parts of the anchor both elastic and plastic failure of soil may occur, dependent on the relative displacement. If the anchor is inclined such as with a grouted anchor, see Figure 4.

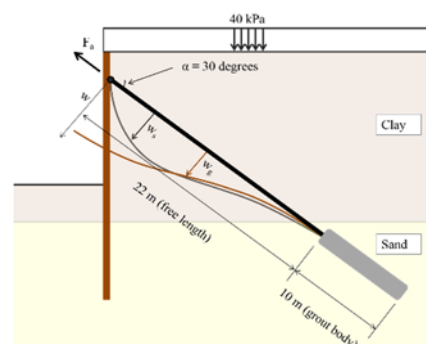


Figure 4: Soil subsidence along the anchor rod (w_g) and the deflection of the anchor rod (w_s) due to settling soil.

The load may increase due to the increase in effective stress. After that due to the diminishing difference and displacement the load may be smaller than in the first meters. As a consequence of the deflection the anchor rod is strained and in addition to the active force (F_a) an increase of the anchor force (ΔF_a) is developed, and a bending moment. Assuming the anchor rod to behave as a series of coupled beam-elements, the internal forces due to the interaction may be calculated. The anchor rod is modelled as four separate parts; for each part the differential equations are established, one of them is visualized in Figure 5. For more details see (Dijkstra, 2015).

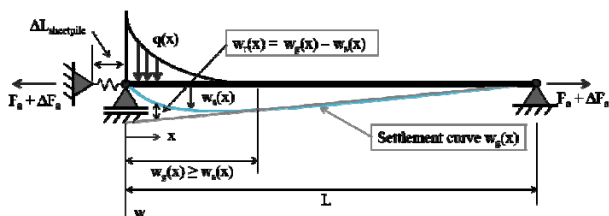


Figure 5: Relative displacement $w_r(x)$ dependent load on the anchor rod. For simplicity of display the beam is sketched horizontally.

The extension of the anchor rod, in combination with its longitudinal rigidity (EA) is determined for the increase in axial force. Eq. 4 represents one part of the anchor rod deflection in which elastic failure of the soil occurs. The flexural stiffness of the anchor rod (EI) and the variable load (q_{var}) are included.

Combining the beams results in Eq. 5 will determine the increase in axial anchor force. The rigidity of the sheet pile wall can be taken into account with use of a linear spring at the support (see Figure 5). Part of the extension of the anchor rod is absorbed by wall deflection in axial direction over a length $\Delta L_{sheetpile}$. Paragraph 3.2 elaborates the impact of the elastic stiffness of a sheet pile wall in greater detail.

Axial interaction of the settling soil with the rod is disregarded. Coupling the various parts enables to solve the interaction for different situation.

$$EI \frac{d^4 w_s}{dx^4} - (F_a + \Delta F_a) \frac{d^2 w_s}{dx^2} + q_{var} w_s = q_{var} w_g \quad (4)$$

$$\Delta F_a = \frac{EA}{L} (\Delta L_1 + \Delta L_2 + \dots - \Delta L_{sheetpile}) \quad (5)$$

2.3 Verification with Embedded piles in Plaxis

To verify the described method of evaluation, for a characteristic situation the same problem was modelled in Plaxis 2D with the anchor modelled as a laterally loaded embedded pile. The interaction between soil and embedded pile row is modelled with a special interface. Although there are limitations to the applicability of an embedded pile with lateral loading, see (Plaxis, 2014), the main purpose of development of the embedded pile was aimed at axial interaction, taking into account proper limits to the interacting forces we were able to model the interaction for a characteristic situation with satisfaction. The results were compared with analytic results based on the model as described in the previous section.

The red line in Figure 6 indicates the result of the analytic equations. If limitation (yellow line) of the lateral load is not present, given as an input for the embedded piles, it may give rise to unrealistic results. Different results can be found giving a limitation to the interaction, see the red line. For more realistic results both the lateral and axial interaction must be limited. After optimization a good corroboration was found between the analytical and numerical results.

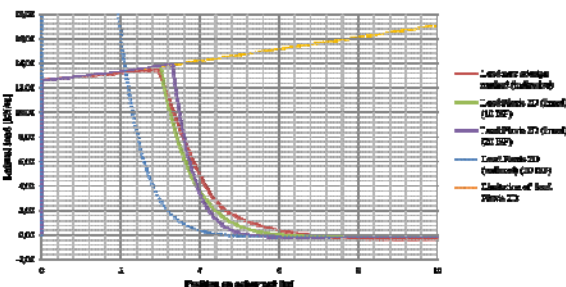


Figure 6: Lateral load on the anchor rod determined with the help of the new design method an Embedded piles in Plaxis 2D.

3 APPLICATION, COMPARISON WITH CUR 166

To display the differences and advantages compared to the conventional method of approach with CUR 166, a situation that is characteristic for a site application was evaluated with the new method and with CUR 166 (case 2) and Plaxis. As a starting point the deflection of the wall was neglected, in a second analysis the effect of the wall was added.

3.1 Anchor rod deformation without roller supports

For this example the anchor rod is positioned with an angle to the vertical and fixed to the wall, as was shown in Figure 4. In this example the settlements are triggered with a surface load. For the analytic approach, the settlement profile was established with a Plaxis 3D analysis, but could also be calculated with different methods, such as Msettle or Plaxis 2D.

As a consequence of the load a settlement of 0,23 m was found at the anchor head, with the depth the settlement will decrease. The clay has the following characteristic parameters; $\gamma = 16 \text{ kN/m}^3$, $\phi' = 20^\circ$ and $c' = 5 \text{ kPa}$. In order to perform the analysis with CUR 166 for the inclined anchor, the “ s_u ”, was established at the middle of the clay layer, ($s_u = 29,5 \text{ kPa}$) with a constant settlement along the beam of 0,23 m (this is one of the limitations of the CUR approach).

Figure 7 indicates the deflection of the anchor. The new approach introduces a settlement dependent load, where the deflection of the anchor rod can't be larger than the settlement of the soil due to the subgrade modulus (which would be unrealistic), contrary to the method indicated in CUR 166.

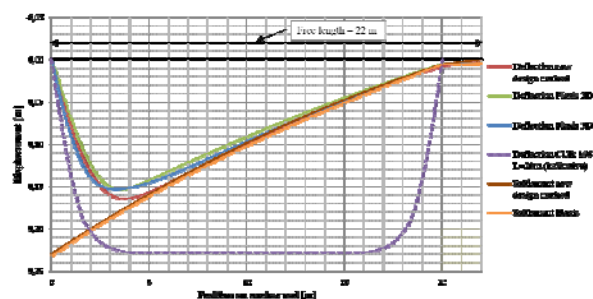


Figure 7: Deflection of the free length of the anchor rod.

Compared to CUR 166, this indicates a smaller increase of the axial forces in the anchor rod. Although it must be mentioned that CUR discounts for the flexibility of the wall, if not the differences might have been even larger. In the updated approach, see the next section, the flexibility is included.

The applied embedded beam element also seems to adequately display a settlement dependent deflection, for that reason the increase in anchor force between the analytic method and Plaxis with embedded beams seems to give a good agreement (see Table 2).

Table 2. Results of the different design methods.

Parameter	CUR 166	New method	Plaxis 2D	Plaxis 3D
Increase axial force ΔF_a	208 kN	72 kN	73 kN	89 kN
Maximum bending moment M_{max}	1,92 kNm	1,70 kNm	1,85 kNm	-

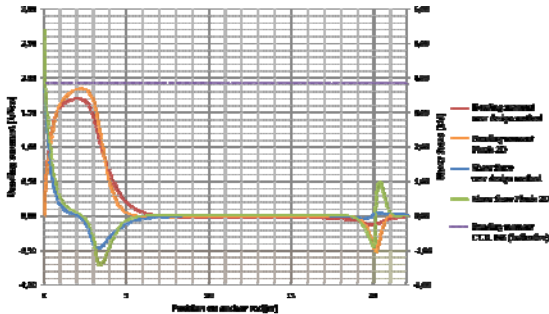


Figure 8: Bending moment and shear force along the free length.

Figure 8 compares the bending moments and shear forces calculated with Plaxis 2D with the new design method. The slight disturbances at 20 m along the anchor rod are caused by the sudden transition of soil characteristic.

The bearing of the soil loading is properly modelled with an elastic model for the beam (the rod). Given the deformation driven behaviour load of settlements the deflection of the anchor rod is limited. For massive and or hollow rods this allows for some plastic redistribution of stresses which enables the optimization of the anchor design, see (Dijkstra, 2015).

3.2 The effect of wall deflection

The extension of the anchor rod by settling soil results in an increase of the axial anchor force. The sheet pile deflects which lessens the elongation and reduces ΔF_a . Eq. 6 indicates this process. The method of evaluation implies to evaluate the center to center distance of the anchor rod (a), the horizontal subgrade modulus (k), the vertical influence length of a deflection, (λ) $\lambda = \sqrt[4]{4EI/k}$, see CUR 166, the perpendicular deflection (u) and the driving horizontal force (ΔF_h).

Figure 9 visualizes in what way the shortening of the anchor rod ($\Delta L_{sheetpile}$) is determined. The corresponding Eq. 7 includes the inclination of the anchor rod (α) and the additional rotation of the rod at the anchor head ($\varphi(0)$).

$$\Delta F_h = a \cdot k \cdot \lambda \cdot u \tag{6}$$

$$\Delta L_{sheetpile} = \frac{\cos(\alpha + \varphi(0))^2 \cdot \Delta F_a}{a \cdot k \cdot \lambda} \tag{7}$$

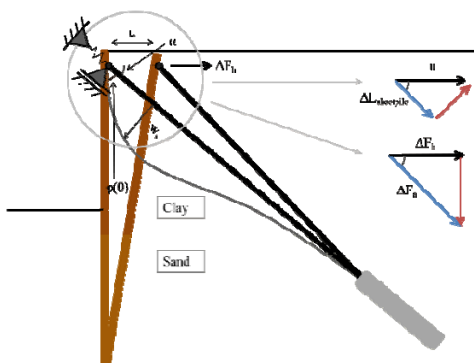


Figure 9: Influence of wall deflection on the deformation of the anchor.

The effect of the increased vertical force in the sheet pile and its resulting movement are not included in the applied method, the same holds for the extra anchor rotation caused by the lateral movement of the rod. Compared to the free length of the anchor rod this rotation is negligible.

The result of including the deflection in the method of evaluation is a further reduction of the increase in axial force, see Table 3.

Table 3. Results of the different design methods with wall deflection

Parameter	CUR 166	New method
Increase axial force ΔF_a	136 kN	53 kN
Maximum bending moment M_{max}	2,17 kNm	1,76 kNm

4 CONCLUDING REMARKS

Due to the limitation in settlement rate for autonomous settlement due to creep, it is important to verify if the interaction is drained or undrained. Due to the low settlement rates the interaction may in practice often be drained, even for clay. In that case the use of the undrained shear strength s_u as a parameter might be judged as peculiar. If the actual shear strength is established accounting for drainage a constant value for the coefficient of influence f_i was found.

The improved method applies a differential equation for parts of the interaction that may be modified to the type of interaction in an iterative way. Contrary to the CUR 166 method the improved method enables to account for more general loading conditions, such as inclined anchors and differences in settlement with depth and various soil conditions in different soil layers.

The validity of the method was verified both with Plaxis calculations in 2D and 3D situations.

Based on a comparison with the renewed model and the Plaxis results it seem that although the CUR 166 is a safe approach it seems more conservative than necessary.

We propose:

For the soil behaviour

- To modify the interaction for clay to $q_z = \tau \cdot D \cdot (1 + f_i)$ where τ is the ultimate shear strength, drained or undrained in combination with a coefficient of influence of $f_i = 8$.

For the steel part

- To establish the anchor force (F_a) based on CUR 166 part 1, chapter 3.
- To calculate the additional anchor force (ΔF_a) with the updated approach as explained in this paper and Dijkstra (2015).
- Check for rotation at the connection ($\epsilon_{max} < \epsilon_u$).

4 REFERENCES

CUR. 2012. CUR 166 Sheetpiling Handbook, 2e ed. Gouda.
 Dijkstra, S. 2015. Soil Settling on anchors, MSc Thesis, Delft University of Technology, (in Dutch)
 Feddema, A., Bredeveld, J., & van Tol, A.F. 2010. Lateral loading of pile foundations due to embankment construction. Num. Methods in Geotechn. Eng. (pp. 631-636). London: Taylor & Francis Group.
 Lottum, H. 2010. Modelonderzoek belasting door zakkende grond op ankerstangen. Deltares.
 Martin, C.M., & Randolph, M.F. 2006. Upper-bound analysis of lateral pile capacity in cohesive soil. Geotechnique 56.2 p. 141-145 .
 Mayne, P.W. 2009. Geomaterial and testing, p. 2777-2872.
 Plaxis. 2014. Pile modelling in a 2D plain strain model. Used on 8 7, 2015, of <http://kb.plaxis.nl/tips-and-tricks/pile-modelling-2d-plain-strain-model>